CHAPTER 3

Methodology

3.1 Research procedure

The Monte Carlo method is a power tool used for solving statistical physics problems. This way involves the calculation the probabilities of a system composed of very many atoms or molecules. Under this system, the equation of motion, which can be expressed mathematically, governs their behaviors. The behavior of entire system often obeys their equations. However, it is impossible to solve these problems exactly. Therefore, we use the Monte Carlo technique to avoid complex mathematics. This chapter devotes the principles and models used to simulate the effects of partial non-polarizable structure on the ferroelectric hysteresis loops. This chapter describes the research procedure in details, that is, various models used in investigating ferroelectric behaviors, preparation the ferroelectric system with partial non-polarizable, calculation hysteresis loop area.

In this work, we use spin models including the DIFFOUR model, modified Heisenberg model with DIFFOUR interaction, and 2D four-state Potts models to simulate ferroelectric thin films with partial non-polarization structure, and then investigate the effects of imperfect structure on ferroelectric hysteresis loops. We start with assigning the Hamiltonian of the DIFFOUR model with an inclusion of non-electric sites as the following equation [36, 38]:

$$H_{DIF} = -\sum_{<ij>}\left(\frac{P_0^2}{2m} - \frac{a}{2}u_i^2 + \frac{b}{2}u_i^4\right) - U\sum_{<ij>}\vec{u}_i \cdot \vec{u}_j - \vec{E}(t)\cdot\sum_i \vec{u}_i, \qquad (3.1)$$

where $P_0^2/2m$ is the kinetic energy, $\vec{u}_i$ denotes the a constant-magnitude vector represented the ferroelectric dipole at site i, a and b are double-well potential parameters, U refers to the ferroelectric interaction, $\vec{E}(t) = E_0\sin(2\pi ft)\hat{z}$ means an

25

external electric field directing only on the z-direction of thin-films, where E_0 and f are field amplitude and field frequency respectively, and $<ij>$ represents the summation taking over the nearest neighbors pairs of dipoles.

If $\left|u_i^\mathrm{r}\right|$ is constant in magnitude (to emphasize effects of domain reorientation), and we use the appropriate reference energy, the Hamiltonian in Equation (3.1) can be rewritten as

$$\mathrm{H}_\mathrm{DIF} = -U \sum_{<ij>} \hat{u}_i \cdot \hat{u}_j - E(t) \sum_i u_{iz}, \tag{3.2}$$

where $\hat{u}_i$ is a unit vector having to one of the possible 14 ferroelectric dipole directions (8 from rhombohedral and 6 from tetragonal structures). The magnitude of each dipole was absorbed into U, and u_{iz} is the z-component dipole at site i. Moreover, U was used as the unit of energy, therefore the unit of temperature T and electric field E were redefined as U/k_B and U respectively, where k_B is the Boltzmann's constant.

In preparing the considered system, the ferroelectric dipoles were assumed to reside in the unit cells the considered ferroelectric lattice system consisting of $N = L \times L \times l$ dipoles, where $L \times L$ denotes a system size and l is the ideal-film thickness (the number of monolayer) and N refers to the total ferroelectric dipoles. The Metropolis algorithm was considered and periodic condition was used along the xy-plane (in-plane direction). Moreover, the number of non-polarizable sites or defect concentration c can vary.

In updating the dipole configuration, a dipole $\hat{u}_i$ was randomly chosen and assigned a new random direction (from possible 14 directions). The new direction was accepted with the following Metropolis probability, p_DIFF,

$$p_\mathrm{DIFF} = \begin{cases} e^{-\Delta \mathrm{H}_i(t)/k_B T} & \text{if } \Delta \mathrm{H}_i(t) > 0 \\ 1 & \text{if } \Delta \mathrm{H}_i(t) \le 0 \end{cases}, \tag{3.3}$$

where $\Delta \mathrm{H}_i(t)$ is the energy difference due to the update at site i and time t. The unit time was scaled in unit of Monte Carlo step per sites (mcs), which is equivalent to N trial updates. The site $\hat{u}_i$ was updated if $\Delta \mathrm{H}_i \le 0$ or random number $r < p_\mathrm{DIFF}$, where $r \in [0,1)$. These procedures were repeated until the simulation terminates.

26

In measuring the observables, a fixed temperature T was chosen since all considered ferroelectric systems are in their ferroelectric phase at this T [34]. Moreover, a given fixed field E_0 was considered to investigate how the other parameters affect the hysteresis behaviors. Therefore, with varying f, and c, the hysteresis loops were drawn by calculating the polarization per dipole, $p(t)$, at time t, i.e.

$$p(t) = \frac{1}{N'} \sum_i u_{iz}(t), \tag{3.4}$$

where $N' = (1-c)N$ is the total number of available dipoles. By varying frequency f, the first 1000 hysteresis loops were discarded for the steady state condition, and next 10000 loops were performed to average the hysteresis area, that is,

$$A = \oint p\, dE, \tag{3.5}$$

and the dynamic order parameter

$$Q = \frac{1}{P} \int_0^P p(t)\, dt, \tag{3.6}$$

where $P = 1/f$ is the field period. Q was used to investigate the dynamic phase transition; $Q \neq 0$ for dynamic ferroelectric phase and $Q = 0$ for dynamic paraelectric phase.

Next, we use the 2D four-state Potts model in simulating the ferroelectric properties due to the coexistence of both 90° and 180° domain wall [60]. Its dipoles have four different alignments and are mutually perpendicular to each other. Therefore, in this work, a two-dimensional array of $N = N_x N_z$ cells on the xz plane was purposed, where N_x and N_z are the number of cells along the x- and z-directions, respectively. Each cell can be also represented by a tetragonal rectangle [61]. A dipole at a cell index i $(0 < i \leq N)$ was replaced by a spin matrix $\hat{S}_i$, which takes one of the four possible directions as the followings

$$\hat{S}_i = \hat{S}_A = \begin{bmatrix} 1 \\ 0 \end{bmatrix} \text{ along } + z \text{ direction (upward)}, \tag{3.7}$$

27

$$\hat{S}_i = \hat{S}_B = \begin{bmatrix} 0 \\ 1 \end{bmatrix} \text{ along } + x \text{ direction (left)}, \tag{3.8}$$

$$\hat{S}_i = \hat{S}_C = \begin{bmatrix} -1 \\ 0 \end{bmatrix} \text{ along } - z \text{ direction (downward)}, \tag{3.9}$$

or

$$\hat{S}_i = \hat{S}_D = \begin{bmatrix} 0 \\ -1 \end{bmatrix} \text{ along } - x \text{ direction (right)} \tag{3.10}$$

where A, B, C or D represents the four possible states. As the direction of the dipole is relevant to the orientation of the tetragonal rectangle, the ferroelastic strain state of a cell can be defined as the following equations [12, 21]

$$\hat{\varepsilon}_i^F = \begin{bmatrix} \varepsilon_0 \\ -\varepsilon_0/2 \end{bmatrix} \text{ (state } A \text{ or } C) \tag{3.11}$$

$$\hat{\varepsilon}_i^F = \begin{bmatrix} -\varepsilon_0 \\ \varepsilon_0/2 \end{bmatrix} \text{ (state } B \text{ or } D) \tag{3.12}$$

where ε_0 is the constant strain of tetragonal cell along the elongated edge.

From a typical 3D tetragonal structure of a perovskite-type ferroelectric material, the positions located at the center of six faces can be represented into a 2D rectangle model with four faces: top, left, bottom, and right. Therefore, the non-polarizable sites were laid at one of possible four sides of a tetragonal cell. At a cell i, the presence of a non-polarizable site can be represented as the following expressions [62, 63]

$$\hat{V}_i = \begin{bmatrix} 0 \\ 0 \end{bmatrix} \text{ (polarizable site)}, \tag{3.13}$$

$$\hat{V}_i = \begin{bmatrix} 1 \\ 0 \end{bmatrix} \text{ (non-polarizable site at top side)}, \tag{3.14}$$

$$\hat{V}_i = \begin{bmatrix} 0 \\ 1 \end{bmatrix} \text{ (non-polarizable site at left side)}, \tag{3.15}$$

28

$$\hat{V}_i = \begin{bmatrix} -1 \\ 0 \end{bmatrix} \text{ (non-polarizable site at bottom side),} \qquad (3.16)$$

$$\hat{V}_i = \begin{bmatrix} 0 \\ -1 \end{bmatrix} \text{ (non-polarizable site at right side).} \qquad (3.17)$$

By considering the mechanical energy density without the anisotropic switching, a ferroelectric material is composed of many energy terms i.e.

$$H_{Potts} = H_{Potts,0} + \sum_i H_{V1} \hat{V}_i^T \hat{S}_i - \sum_{<ij>} H_{V2} \{\hat{V}_i^T \hat{V}_j\}\{\hat{S}_i^T \hat{S}_j\}, \qquad (3.18)$$

where $H_{Potts,0}$ is the Hamiltonian of a spin system with any polarizable sites, $<ij>$ is the summation over the nearest neighbors, H_{V1} refers to the coupling interaction between non-polarizable sites and dipoles, H_{V2} is the coupling strength between the distorted cells and the neighboring dipoles. $\hat{X}^T$ is the transpose matrix of $\hat{X}$ which has the following form $\hat{X} = \begin{bmatrix} X_z \\ X_x \end{bmatrix}$, where X_z and X_x are the components along to z- (longitudinal) and x- (transverse) directions, respectively ($\hat{X} = \hat{V}$ or $\hat{S}$). Its unit is absorbed into H_{V1} or H_{V2}, and each term in Equation (3.18) was also redefined as the energy unit. For the presence of polarizable sites, the Hamiltonian of system can be written as

$$H_{Potts,0} = -\sum_{<ij>} J\hat{S}_i^T \hat{S}_j - P_S \sum_i \hat{E}_i^T \hat{S}_i - \alpha \sum_{<ij>} \hat{\varepsilon}_i^{FT} \hat{\varepsilon}_j^F - \sum_i \hat{\sigma}^T \hat{\varepsilon}_i, \qquad (3.19)$$

where J and α are the dipole-coupling coefficient and ferroelastic-strain-coupling coefficient, respectively, P_S is the magnitude of the dipole moment of a cell, $\hat{E}$ and $\hat{\sigma}$ are the periodic external electric and stress fields. Similarly, J and α are redefined as the energy unit by absorbing the unit of $\hat{S}$ and $\hat{\varepsilon}$, respectively. Therefore, the unit of the electric field was defined as J and temperature as J/k_B, where k_B is the Boltzmann's constant. If both external electric and stress fields are uniform in space, and have only longitudinal forms (z-direction) and initially in phase, they can be expressed as

$$\hat{E} = \begin{bmatrix} E_z \\ E_x \end{bmatrix} = \begin{bmatrix} E_0 \sin(2\pi f_E t) \\ 0 \end{bmatrix}, \tag{3.20}$$

and

$$\hat{\sigma} = \begin{bmatrix} \sigma_z \\ \sigma_x \end{bmatrix} = \begin{bmatrix} \sigma_0 \sin(2\pi f_\sigma t) \\ 0 \end{bmatrix}, \tag{3.21}$$

where E_0 and σ_0 are the electric and stress field amplitudes, for a tensile stress, $\sigma_z = \sigma_0$ ($\sigma_0 > 0$ for a tensile stress and $\sigma_0 < 0$ for a compressive stress), t is the time which is scaled in term of number of Monte Carlo steps (mcs), f_E and f_σ are the electric and stress field frequencies, respectively, which have the unit of mcs^{-1}. In the simulation, the numbers of data (or points) per a loop used to generate a hysteresis loop rely on one field frequency (or one period). Under a static and periodic field, a hysteresis loop can be created easily by these points. However, two different field frequencies may lead to their different numbers of points per a loop. This is not quite suitable to plot a hysteresis loop and compare using different numbers of points. Therefore, in this work, $f_E = f_\sigma = f$ as previous works [20, 64]. In Equation (3.19), $\hat{\varepsilon}_i$ is the total strain which can be divided into two parts (without field-induced strain) as

$$\hat{\varepsilon}_i = \hat{\varepsilon}_i^F + \hat{\varepsilon}_i^{el} \tag{3.22}$$
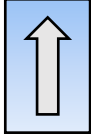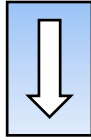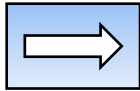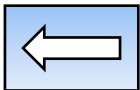
where $\hat{\varepsilon}_i^{el}$ is the elastic strain determined by the elastic property of the material. For a small stress, it was found that

$$\hat{\varepsilon}_i^{el} = \frac{1}{Y} \begin{bmatrix} 1 & -\upsilon \\ -\upsilon & 1 \end{bmatrix} \begin{bmatrix} \sigma_z \\ \sigma_x \end{bmatrix}. \tag{3.23}$$

Here, Y and υ are the Young's modulus and Poisson ratio, respectively.

In preparing the system, each spin was placed at any sites randomly with possible directions as described previously. Consequently, the system was initially unpoled. The ferroelastic strain states were also automatically initialized since both spin states and ferroelastic strain states were associated as Equations (3.7) – (3.12) (see Table 3.1).

Table 3.1 Possible four directions of a dipole and possible two strain states

Dipole	Direction	Strain
$\hat{S}_A = \begin{bmatrix} 1 \\ 0 \end{bmatrix}$	$+z$	$\hat{\varepsilon}^F = \begin{bmatrix} \varepsilon_0 \\ -\varepsilon_0/2 \end{bmatrix}$
$\hat{S}_C = \begin{bmatrix} -1 \\ 0 \end{bmatrix}$	$-z$	
$\hat{S}_B = \begin{bmatrix} 0 \\ 1 \end{bmatrix}$	$+x$	$\hat{\varepsilon}^F = \begin{bmatrix} -\varepsilon_0 \\ \varepsilon_0/2 \end{bmatrix}$
$\hat{S}_A = \begin{bmatrix} 0 \\ -1 \end{bmatrix}$	$-x$	

In simulating the existence of non-polarizable sites, the total number of non-polarizable sites $N_V = cN$, where c is the non-polarizable probability or defect concentration, was defined where, for each cell, the non-polarizable sites randomly distributed on possible positions as mentioned in Equations (3.13) − (3.17) (see Figure 3.1). The presence of non-polarizable site at possible four sides of a cell is governed by the probability p_T (top), p_B (bottom), p_L (left) and p_R (right). These probabilities follow the condition $p_T + p_L + p_B + p_R = 1$. Moreover, periodic and free boundary conditions were employed along x- and z-directions, respectively.
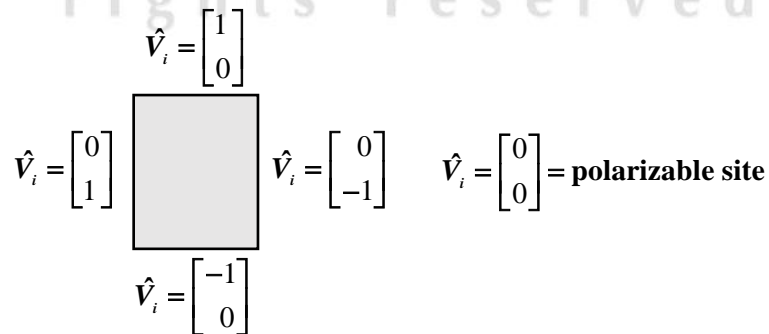

Figure 3.1 Non-polarizable sites on possible 4 sides of a 2D-tetragonal cell.

31

After providing the initial configuration of system, a spin was randomly selected for a trial rotation which is determined by the Metropolis algorithm [65]. The macroscopic polarization and strain were calculated using the following expressions:

$$P_z = \frac{P_S \sum_i \hat{n}^T \hat{S}_i}{N},$$
(3.24)

$$\varepsilon_z = \frac{\sum_i \hat{n}_i^T (\hat{\varepsilon}_i - \hat{\varepsilon}_i^0)}{N},$$
(3.25)

and

$$\varepsilon_x = \frac{\sum_i \hat{q}^T (\hat{\varepsilon}_i - \hat{\varepsilon}_i^0)}{N},$$
(3.26)

where $\hat{n} = \begin{bmatrix} 1 \\ 0 \end{bmatrix}$ and $\hat{q} = \begin{bmatrix} 0 \\ 1 \end{bmatrix}$ denote the longitudinal and transverse unit matrix, respectively, and $\hat{\varepsilon}_i^0$ is the initial strain matrix for each cell. Then the ferroelectric hysteresis loops were obtained to investigate their properties through the hysteresis area as Equation (3.5).

3.2   The single histogram method

The single histogram method allows us to extrapolate some results to nearby temperatures of a single Monte Carlo simulation performed at a given temperature T_0. The idea of using the single histogram method is to extract some results from a single Monte Carlo simulation at a given temperature. The aim of the single histogram method is to obtain one function at one temperature from a simulation at another temperature.

We have shown that the estimator of an observable Q_M from measurements M can be expressed as

$$Q_M = \frac{\sum_{i=1}^{M} Q_{\mu_i} p_{\mu_i}^{-1} e^{-\beta E_{\mu_i}}}{\sum_{j=1}^{M} p_{\mu_j}^{-1} e^{-\beta E_{\mu_j}}},$$
(3.27)

where the energies E_{μ_i} are the total energies of the state μ_i and not energies per spin.

32

In most simulations, p_{μ_i} is the Boltzmann probability for a considered temperature. However, for another temperature, we may choose it to be $p_{\mu_i} = \frac{e^{-\beta_0 E_{\mu_i}}}{Z_0}$, where $\beta_0 = 1/k_B T_0$. Then, we obtain a fundamental equation of the histogram method, that is,

$$Q_M = \frac{\sum_{i=1}^{M} Q_{\mu_i} e^{-(\beta-\beta_0)E_{\mu_i}}}{\sum_{j=1}^{M} e^{-(\beta-\beta_0)E_{\mu_j}}}. \qquad (3.28)$$

To avoid using every raw data of Q_{μ_i} and E_{μ_i}, we replace them with the two-dimensional histogram $N(E,Q)$ which is the number of times during the Monte Carlo run at a state with the energy E and observable Q (for example, magnetization). Thus Equation (3.28) becomes

$$Q_M = \frac{\sum_{E,Q} Q N(E,Q) e^{-(\beta-\beta_0)E}}{\sum_{E,Q} N(E,Q) e^{-(\beta-\beta_0)E}}. \qquad (3.29)$$

However, it is unworkable to fit the histogram with the extensive observables such as E and Q. Therefore, we perform the sums overs Q first and use one-dimensional arrays to keep the average Q as a function of E, that is,

$$Q_M(\beta) = \frac{\sum_E \langle Q(E) \rangle N(E) e^{-(\beta-\beta_0)E}}{\sum_E N(E) e^{-(\beta-\beta_0)E}}. \qquad (3.30)$$

We perform the summation in logarithmic terms instead of the summation of exponential function in Equation (3.30) to avoid overflow in computer. To do this, let ℓ_1 and ℓ_2 be the logarithms of x_1 and x_2 and $\ell_1 \geq \ell_2$, then

$$\begin{aligned} \ln(x_1 + x_2) &= \ln(e^{\ell_1} + e^{\ell_2}) \\ &= \ln[e^{\ell_1}(1 + e^{\ell_2 - \ell_1})] \\ &= \ell_1 + \ln(1 + e^{\ell_2 - \ell_1}). \end{aligned} \qquad (3.31)$$

Equation (3.31) can be safety evaluated without overflow because $e^{\ell_2 - \ell_1} < 1$. (For very small x, we can use a function called log1p() in C to evaluate $\ln(1+x)$.). Thus, we can calculate Q_M in Equation (3.30)

33

$$Q_M = \frac{\text{numerator}}{\text{denominator}} = e^{\ln(\text{numerator}) - \ln(\text{denominator})}. \tag{3.32}$$

However, we cannot take the logarithms of some observables that may be negative, such as energy or magnetization. To avoid this problem, we shift their values with a constant value that is large enough to make them positive.

3.3   Estimation of power-law exponents

As described in section 2.2, hysteresis area can be written in the power-law terms, that is, hysteresis area is a function of some parameters with their exponents. We can estimate these exponents to find out how they effect on hysteresis area A. In this section, we will show how to estimate the exponents in details.

Firstly, consider a variable A be a function of three parameters: X, Y and Z. We can write it in the power-law terms, that is,

$$A = kX^{\alpha}Y^{\beta}Z^{\gamma}, \tag{3.33}$$

where k is a constant, α, β, and γ are the exponents of X, Y, and Z, respectively. Next, we take the (base-ten) logarithm of both sides of Equation (3.33) and use the most basic property of logarithm. This yields

$$\log A = \log k + \alpha \log X + \beta \log Y + \gamma \log Z. \tag{3.34}$$

To estimate the exponent α, we let Y and Z be two constants, therefore Equation (3.34) becomes

$$\log A = \alpha \log X + B, \tag{3.35}$$

where

$$B = \beta \log Y + \gamma \log Z + \log k. \tag{3.36}$$

If we define $y = \log A$, $x = \log X$, $m = \alpha$ and $c = B$ and substitute them into Equation (3.35), we get a linear equation of two variables y and x, that is, $y = mx + c$, where m is the slope or gradient of a line and c denotes the y-intercept—a point at which a line crosses the y-axis. This means if we plot $\log A$ versus $\log X$, we should obtain a

34

straight line and can estimate the value of α by calculating the line's slope in the usual way, that is, for

$$\alpha = \frac{\log A_2 - \log A_1}{\log X_2 - \log X_1}. \tag{3.1}$$

We can also find the value of the y-intercept by substituting $\log X = 0$ (or $X = 1$), that is, $B = \log A$.

Next, if we choose X and Z be two constants, Equation (3.34) yields

$$\log A = \beta \log Y + C, \tag{3.38}$$

where

$$C = \alpha \log X + \gamma \log Z + \log k. \tag{3.39}$$

In the same way, if we plot $\log A$ versus $\log Y$, we can estimate the exponent β by calculating the line's slope, that is,

$$\beta = \frac{\log A_2 - \log A_1}{\log Y_2 - \log Y_1}, \tag{3.40}$$

and if $\log Y = 0$, we get $C = \log A$. Finally, if X and Y are two constants, we get

$$\log A = \gamma \log Z + D, \tag{3.41}$$

where

$$D = \alpha \log X + \beta \log Y + \log k. \tag{3.2}$$

We can find the exponent γ by plotting $\log A$ versus $\log Z$, i.e.,

$$\gamma = \frac{\log A_2 - \log A_1}{\log Z_2 - \log Z_1}, \tag{3.43}$$

and if $\log Z = 0$, this yields also $D = \log A$.

Now, we can use the exponents α, β, and γ to fit a model using linear regression analysis. However, we need to determine how well the model fits the data. In statistics,

35

we use R-squared or R^2 to show a goodness-of-fit statistics. R^2 is a statistical measure of how close the data are to the fitted regression line. In general, R^2 is always between 0 to 1. The closer to 1 the R^2, the better the model fits our data. We can get the R^2 from many statistical software.